3rd International Symposium on Two-Phase Flow Modelling and Experimentation
Pisa, 22-24 September 2004

THE EFFECT OF THE STRUCTURAL EVOLUTION OF SNOW ON HEAT TRANSFER

Th. U. Kaempfer, S. A. Sokratov, M. Schneebeli

WSL, Swiss Federal Institute for Snow and Avalanche Research
Flüelastrasse 11, 7270 Davos, Switzerland
E-mail: kaempfer@slf.ch

ABSTRACT

The heat flow through a snow cover profoundly changes its structure and thus the thermophysical and mechanical properties of snow. Despite the great amount of empirical data collected so far, the physical processes behind these changes are poorly understood because snow sinters and recrystallizes simultaneously at temperatures typical on earth. Heat conduction in snow takes place as (i) conduction in the ice matrix and pore space, (ii) heat transport by water vapor diffusion, and (iii) latent heat release and gain due to phase changes. X-ray computed micro-tomography allows detailed representations of the 3D-microstructure of snow and its evolution during metamorphism without disturbing the snow sample. The reconstructed microstructure of snow was used to simulate the heat conduction in the ice matrix of snow and its evolution during controlled temperature gradient metamorphism. The numerical results, compared with the measured effective heat conductivites of the snow samples, suggest the relative contribution of the components of the heat flux through snow to be considerably different from what is assumed nowadays.

1 INTRODUCTION

Evolution of thermophysical properties of natural snow, affecting the soil temperature regime and the soil-atmosphere interaction, is an important topic in modeling the energy balance of snow-covered landscapes [1]. In climate models, the natural snow cover is usually characterized by the spatial and temporal variation of its "effective" parameters. The primary one for the energy balance is the effective heat conductivity of the snow pack [2].

Snow cover models account for the layered structure of a snow pack and estimate the heat fluxes through snow based on the local vertical variability of the properties of the individual snow layers [3; 4]. Key parameters in each layer are snow density, grain size, and crystal type.

Heat flux through snow is governed by heat conduction in the ice matrix, heat conduction in the pore space, and the heat associated with water vapor diffusion in the pore space. The latter divides into the actually transferred heat (heat capacity of the transfered water vapor) and the latent heat release and gain due to alternating evaporation and sublimation at the ice matrix-pore interfaces [5]. So far, it is assumed that the heat is mainly transported through the ice matrix and thus that the effective heat conductivity of snow (EHC) mainly depends on the snow density [6]. However, measured EHC differs up to 5 times between measurements made in snow similar both in density and in crystal type [6; 7]. This large scatter is believed to be associated with water vapor diffusion in the pore space of snow [6] and the microstructure.

The experimental data on the water vapor diffusion, in terms of the effective water vapor diffusion coefficient (EDC) in snow, also shows about 5 times difference from experiment to experiment [8]. Moreover, most of the reported values of EDC are much higher than in free air, despite the fact that only the pore space is available for the mass transfer. This is related to possibly enhanced temperature gradients in the pore space relative to those in the ice matrix, due to the large difference in the heat conductivity of air and ice [9]. Nevertheless the heat transported by this presumably enhanced water vapor diffusion was still estimated to be negligibly small relative to the overall heat flux [10].

Regardless of the experimental method, the published EHC values were provided by substitution of measured temperature gradients or temperature changes with time into equations based on the Fourier law of heat conduction. The EDC was also calculated in a similar way (Fick's law), with the assumption that the water vapor is saturated in the pore space and the flux is regulated by an applied temperature gradient.

The uncertainties listed above suggest that either the interrelation between the components of the heat transfer is treated wrongly, or that the mechanism of water vapor diffusion has some aspects being missed in the presently available constructions.

The other problem is the representation of the snow microstructure [9]. Until now, its complexity in real snow always requires simplification of the snow geometry, which could also be the reason for the unexplained differences between the results based on theoretical constructions and the experiments.

In this work, a finite element model of heat conduction in the ice matrix based on the tomographic images of the actual ice and pore distribution in the studied snow samples was constructed. The microstructure was imaged at regular time intervals during temperature gradient metamorphism and the numerical model was applied to the evolving structure. The computational thermal history was compared to the measured EHC of the sample. The result showed that the change in heat conductivity in the ice matrix was opposite to the observed EHC. The modification of the microstructure during temperature gradient metamorphism caused strong changes in the processes of heat conduction in the pores, and much less in the ice matrix. This result is contrary to

(a)

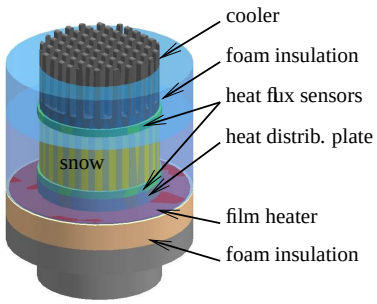

(b)

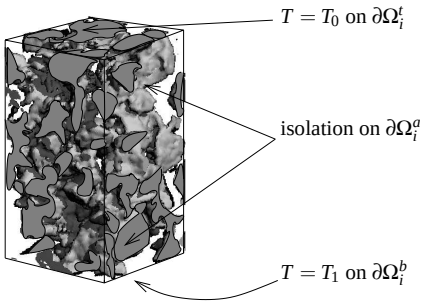

Figure 1. The temperature-controlled snow breeder (a). The snow-chamber had a diameter of 50 mm and a height of 23 mm. (b) The subdomain (2.5 × 2.5 × 4.75 mm) used for the numerical computations.

previous assumptions.

2 MODEL

2.1 Experimental and numerical setup

A snow sample was sieved into a sample container (Fig. 1 (a)) and subjected to a temperature gradient of 40 K m^{-1} in the vertical direction by controlling the temperature at the bottom and top of the sample. The snow was imaged by X-ray computed micro-tomography every eight hours at the same spatial location with a resolution of 25 μm and without disturbing the sample during 14 days. Simultaneously, two heat flux sensors at the top and bottom of the container measured the heat transfer across the snow sample. A more detailed description of the experimental setup is presented in [5].

The imaged domain of the snow sample was directly used to construct the computational domain. In a volume, Ω, of $100 \times 100 \times 190$ voxels, the digitized ice matrix, Ω_i, was extracted (Fig. 1 (b)) and meshed by transforming each ice-voxel to an eight-node brick finite element. Denote the boundary of the compuational domain Ω_i by $\partial\Omega_i$ and set $\partial\Omega_i = \partial\Omega_i^t \cup \partial\Omega_i^b \cup \partial\Omega_i^a$, where the superscripts t and b stand for the top and bottom of Ω_i and $\partial\Omega_i^a$ represents the side boundary as well as all the ice-aire interfaces inside the volume Ω.

2.2 Mathematical model and numerical solution

In order to determine the importance of the heat conduction through the ice matrix with respect to the overall heat transport in snow, the energy conservation equation within the ice matrix was solved. A scale analysis by Christon [11] showed that the temperature gradient metamorphism is quasi-steady, the only significant transient being the movement of the solid-vapor interface with time. Thus, in the ice matrix, the energy conservation is supposed to be steady. Moreover, there are very few defects in the crystal structure of snow crystals [12] and the thermal properties are those of pure ice.

The boundary conditions at the top and bottom of the computational domain were of Dirichlet type and fixed such that a linear temperature distribution would lead to the same temperature gradient as imposed in the experiment. On all the other domain boundaries, homogeneous Neumann boundary conditions were applied, thus supposing isolation at the outer walls of the cylinder (as in the experiment) and no heat exchange between ice and air, which corresponded to neglecting the pore space.

This resulted in the following problem to be solved on the ice matrix:

$$\begin{cases} k_i \Delta T = 0 & x \in \Omega_i, \\ T = T_0 & x \text{ on } \partial\Omega_i^t \\ T = T_1 & x \text{ on } \partial\Omega_i^b \\ \frac{\partial T}{\partial n} = 0 & x \text{ on } \partial\Omega_i^a, \end{cases} \tag{1}$$

where k_i is the conductivity of ice supposed to be constant, T represents the temperature depending on the position x, and T_0 and T_1 are the imposed boundary conditions at the top and bottom of the sample, respectively.

The finite element code by van Rietbergen *et al.* [13], initially designed for deformation computations in trabecular bone [14], has recently been used for elastic stress simulations in snow [15]. For the present work, the program was adapted to solve the energy conservation problem given in Eq. (1) by using the physical analogies [16] between the Hooke's and Fourier's laws.

After the discretization of the problem, the linear system of equations was solved by a preconditioned conjugate gradient method together with an element-by-element method [13; 14].

2.3 Representative sample-volume

In order to limit computational time, the domain Ω was chosen as small as possible, but such that the volume is still large enough to represent the characteristics of the snow sample, in particular its density. The representative elementary volume (REV) [17] is a measure for this needed volume. The ice-voxel fraction within sub-volumes of increasing size around the center of the domain Ω was calculated. The changes in ice fraction, which is proportional to the snow density, as a function of the sub-volume size is represented in Fig. 2 for the sample at days $0, 3, 6, 9$, and 12. The choice of our computational domain with $100 \times 100 \times 190$ voxels is about two times larger than the minimal REV with respect to the density. The REV with respect to temperature is more difficult to estimate.

3 RESULTS AND DISCUSSION

3.1 Microstructural evolution

The microstructural evolution during the whole temperature gradient metamorphism experiment has been observed (Fig. 3).

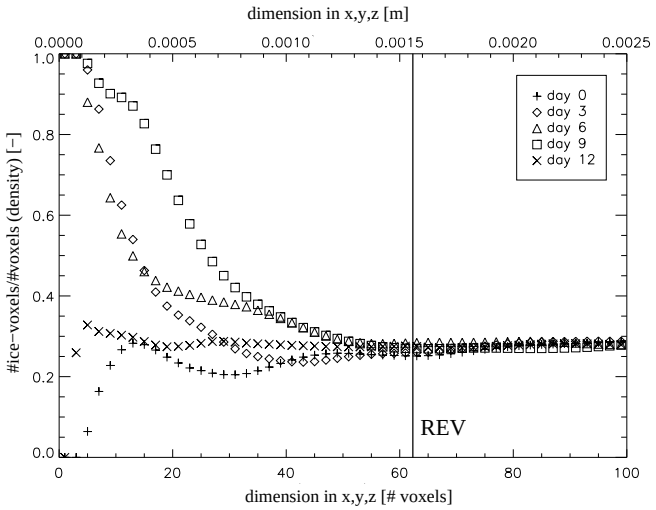

Figure 2. The fraction of ice-voxels, which is proportional to the density, in function of the size of cubic sub-volumes of the computational domain Ω, for the microstructure every three days during the experiment.

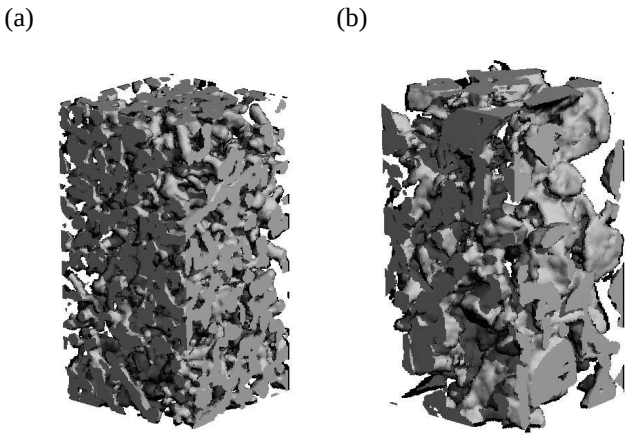

Figure 3. The microstructural evolution of the snow sample is observed by micro-tomography. The structure of the initial snow (a) and after 14 days of temperature gradient metamorphism with a gradient of 40 K m^{-1} (b). The represented volume is 2.5 $\times$ 2.5 $\times$ 4.75 mm, observed with a spacial resolution of 25 μm.

A general coarsening of the structure occurs, while the density remains quasi constant (Fig. 2).

3.2 Temperature distribution

The temperature distribution within the ice matrix, neglecting the porous space and any phase change, was computed on the structures obtained form the tomographic imaging (Figs. 4 and 5 at the beginning and the end of the experiment, respectively). The minimum, maximum, and mean temperatures in each x,y-plane along the z-direction of the computational domain (Figs. 6 and 7) were also compared.

While at the beginning of the experiment (Fig. 4) the temperature distribution is very close to a linear one, which would be expected for a homogenous structure, it gets more and more irregular towards the end of the experiment (Fig. 5). This observation is also supported by comparing the minimum, maximum, and mean temperatures in each x,y-plane along the z-direction of the computational domain (Figs. 6 and 7).

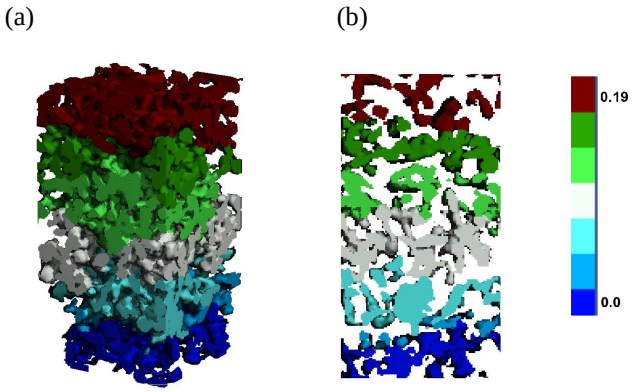

Figure 4. Computed temperature distribution across the ice matrix of the sample (a) and through the midsection in the y,z-plane, 10 voxels thick (b), computed with the structure of day 0.

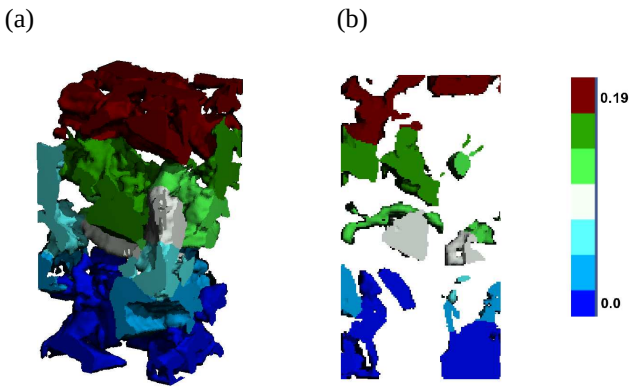

Figure 5. Computed temperature distribution across the ice matrix of the sample (a) and through the midsection in the y,z-plane, 10 voxels thick (b), computed with the structure of day 14.

3.3 Temperature gradients

Based on the temperature field, the temperature gradient within the ice matrix was determined. For each x,y-plane along the z-direction of the computational domain, the maximum and mean gradients are represented for the initial (Fig. 8) and final (Fig. 9) snow structures. The minimum gradients (not shown) are close to zero throughout the structures.

The computed mean temperature gradient within the ice matrix was smaller than the effectively applied temperature gradient (Figs. 8 and 9), due to the tortuosity of the ice matrix. Moreover, a high variation of this gradient was observed. This is explained by the irregularity of the microstructure. The same quantity of heat (because imposed) has to flow alternately through thick or thin ice branches. Moreover, the variation of the temperature gradient increased slightly from day 0 to day 14.

3.4 Heat conductivity

The heat conductivity in the ice matrix through the snow sample was determined based on the computed temperature gradients. The comparison of this ice-only conductivity with the measured effective heat conductivity through the snow sample is presented in Fig. 10.

While the EHC increases, the ice matrix heat conductivity

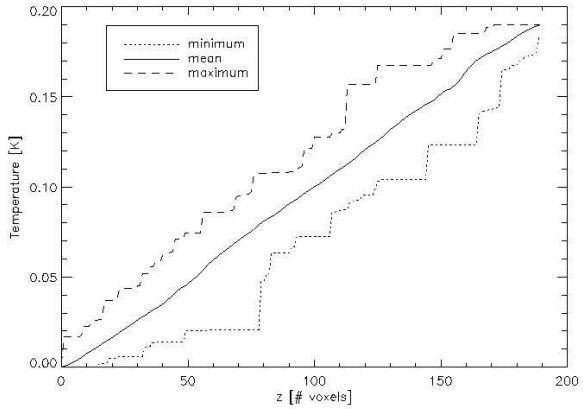

Figure 6. For each x, y-voxel plane, along the z-direction, the minimum, maximum, and mean temperatures, computed for the ice matrix of the sample at day 0.

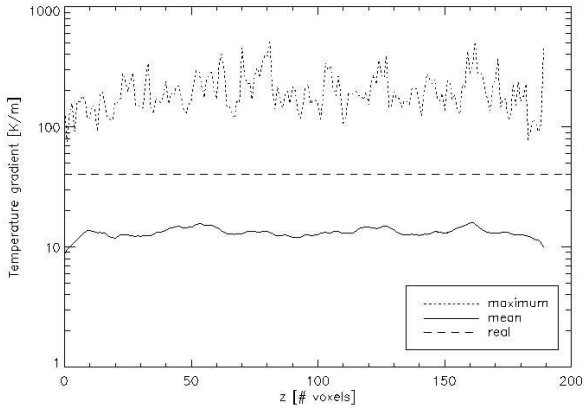

Figure 8. For each x, y-voxel plane, along the z-direction, maximum and mean computed temperature gradients for the ice matrix of the sample at day 0. The overall applied temperature gradient was 40 K m^{-1}.

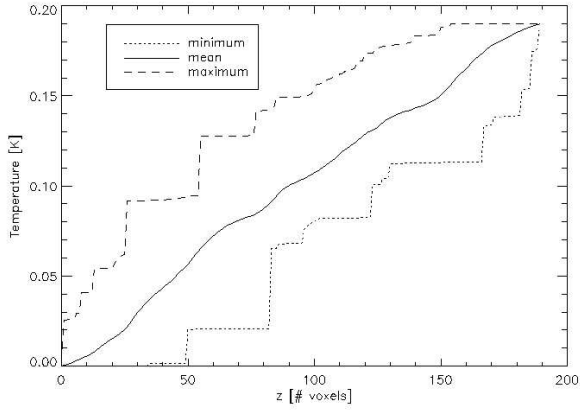

Figure 7. For each x, y-voxel plane, along the z-direction, the minimum, maximum, and mean temperatures, computed for the ice matrix of the sample at day 14.

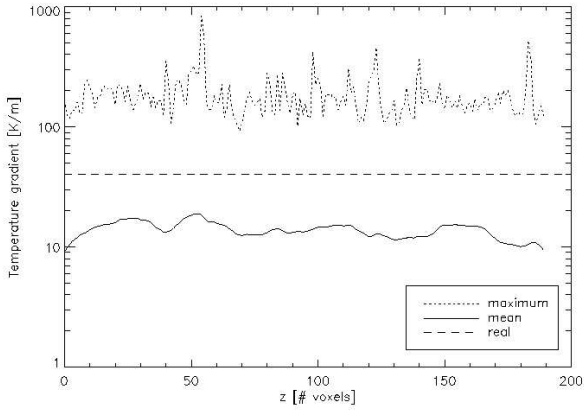

Figure 9. For each x, y-voxel plane, along the z-direction, maximum and mean computed temperature gradients for the ice matrix of the sample at day 14. The overall applied temperature gradient was 40 K m^{-1}.

decreases. This indicates that the weights of the different contributions to heat transfer through snow depend on the snow microstructure and thus change during snow metamorphism.

4 CONCLUSION

Using the real snow structures in the modeling of the heat fbw through snow (the "macro-scale" heat transfer) showed that the conduction in the ice matrix alone contributes less than 30% to the overall heat flux (Fig. 10). Since the water vapor flux itself does not transport much heat either, the key in relating the results of numerical simulations by conduction models to the actually observed heat fluxes and EHC lies in the energy exchange between the ice matrix and the pore air.

Including this term in modeling the heat transfer through snow, with separating the temperatures of the ice surface and of the pore air [18], faces the necessity of relating the reported experimental data on the evaporation coefficient of ice to the convection mass transfer coefficient (and based on the mass and heat transfer analogy to the convection heat transfer coefficient) of snow. Observations of the actual evolution of snow geometry under controlled environmental conditions by computed X-ray micro-tomography can be used for the estimation of these coefficients.

According to the results presented above, the representative volume for the macro-scale heat transfer in snow is in the order of 1.5 mm. Note that this order corresponds to the thickness of the minimal layers found in natural snow packs [19]. The size of the representative volume implies that the resolution of a model describing the macroscopic heat flux cannot be finer than that. On the other hand, the high variabilities of the temperature and its gradient at the micro-scale, even without the effects of latent heat release and gain at the ice matrix surface, suggest that accounting for the convective heat and mass exchange in a heat transfer model, and especially attempts at modeling snow metamorphism, would require higher resolution and accounting for the direction of the mass and heat fluxes at the ice matrix surface (the micro-scale heat transfer). An accurate parameterization of the micro-scale processes for incorporation into a macro-scale heat transfer model would also require the use of the real snow geometry as presented by the X-ray computed micro-tomography.

The discrepancies between the previously accepted theoretical constructions and the results of the experimental measurements of EHC and EDC (see section 1) can be explained by improper scaling of the components of the heat transfer and by

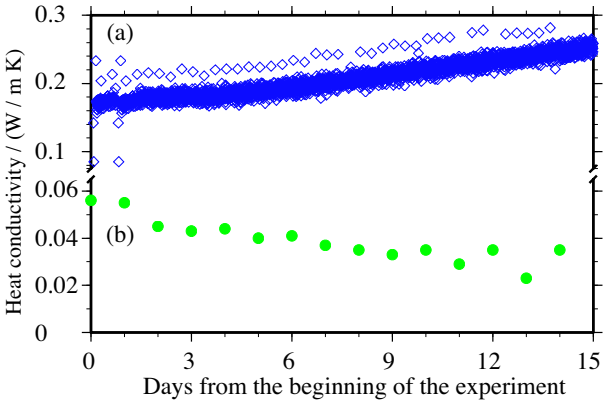

Figure 10. Evolution of the measured effective heat conductivity of the snow sample (a) compared to the computed virtual heat conductivity considering the ice matrix only (b).

non-accounted convective heat exchange at the ice matrix surface [20]. The work on combining the new description of the heat transfer in snow with the snow geometry as observed by the X-ray computed micro-tomography will be a next milestone in snow metamorphism modeling.

ACKNOWLEDGMENT

Special thanks are to B. van Rietbergen for the finite element program, which served as a basis for the presented computations. The financial support of Swiss National Science Foundation (Project No. 200021-100294) is appreciated.

NOMENCLATURE

k_i Conductivity of ice [W m^{-1} K^{-1}]
T Temperature [K]
Ω_i Computational domain
$\partial\Omega_i$ Boundary of domain
a Ice-aire interface (superscript)
b Bottom (superscript)
t Top (superscript)

REFERENCES

[1] S.A. Sokratov and R.G. Barry, Intraseasonal variation of the thermoinsulation effect of snow cover on soil temperatures and energy balance, *J. Geophys. Res.*, vol. 107(D10), doi:10.1029/2001JD000489, 2002

[2] V. Bugnion and P.H. Stone, Snowpack model estimates of the mass balance of the Greenland ice sheet and its changes over the twentyfist century, *Clim. Dyn.*, vol. 20(1), pp. 87–106, 2002

[3] P. Bartelt and M. Lehning, A physical SNOWPACK model for the Swiss avalanche warning—-Part I: Numerical model, *Cold Reg. Sci. Technol.*, vol. 35(3), pp. 123–145, 2002

[4] Brun, E., David, P., Sudul, M. and Brunot, G., A numerical model to simulate snow-cover stratigraphy for operational avalanche forecasting, *J. Glaciology*, 38(128), pp. 13-22, 1992

[5] S. A. Sokratov and M. Schneebeli, Heat conduction and microstructural evolution of snow during temperature gradient metamorphism, *Env. Sci. and Technol.*, 2004, submitted.

[6] M. Sturm, J. Holmgren, J. König, and K. Morris, The thermal conductivity of seasonal snow, *J. Glaciology*, 43(143), pp. 26-41, 1997

[7] M. Sturm, D.K. Perovich and J. Holmgren, Thermal conductivity and heat transfer through the snow on the ice of the Beaufort Sea, *J. Geophys. Res.*, 107(C10), 8043 doi:10.1029/2000JC000409, 1997

[8] S.A. Sokratov and N. Maeno, effective water vapor diffusion coefficient of snow under a temperature gradient, *Water Resources Res.*, vol. 36(5), pp. 1269–1276, 2002

[9] S.C. Colbeck, The vapor diffusion coefficient for snow, *Water Resources Res.*, vol. 29(1), pp. 109–115, 1993

[10] M.R. Albert and W.R. McGilvary, Thermal effects due to air fbw and vapor transport in dry snow, *J. Glaciology*, vol. 38(129), pp. 273–281, 2002

[11] M. Christon, 3-D Transient Microanalysis of Multi-Phase Heat and Mass Transport in Ice-Lattices, Ph.D. thesis, Colorado State University, Fort Collins, CO., 1990

[12] M. Christon, P. J. Burns and R. A. Sommerfeld, Quasi-steady temperature gradient metamorphism in idealized, dry snow, *Numer. Heat Transfer, Part A* vol. 25(3), pp. 259-278, 1994

[13] B. van Rietbergen, H. Weinans, R. Huiskes, and A. Odgaard, Computational strategies for iterative solutions of lare FEM applications employing voxel data. *Internat. J. Numer. Meth. Engrg.*, vol. 39 (16), pp. 2743-2767, 1996

[14] B. van Rietbergen, H. Weinans, R. Huiskes, and B.J.W. Polman, A new method to determine trabecular bone elastic properties and loading using micromechanical finite-element models. *J. Biomech.*, vol. 28(1), pp. 69-81, 1995

[15] M. Schneebeli, Numerical simulation of elastic stress in the microstructure of snow, *Ann. of Glaciology*, vol. 38, 2004, in press.

[16] H. F. Wang and M. P. Anderson, *Introduction to Groundwater Modeling, Finite Difference and Finite Element Methods*, W. H. Freeman and Company, San Francisco, 1982

[17] G. O. Brown and H. T. Hsieh, Evaluation of laboratory dolomite core sample size using representative elementary volume concepts, *Water Resources Res.*, Vol. 36(5), pp. 1199-1207, 2000

[18] P. Bartelt, O. Buser and S.A. Sokratov, A non-equilibrium treatment of heat and mass transfer in alpine snowcovers, *Cold Regions Sci. Technol.*, vol. 39, 2004, in press.

[19] C. Pielmeier and M. Schneebeli, Stratigraphy and changes in hardness of snow measured by hand, rammsonde, and snow micro penetrometer: A comparison with planar sections, *Cold Regions Sci. Technol.*, vol. 37(3), pp. 393-405, 2003

[20] F. P. Incropera and D. P. DeWitt, *Fundamentals of Heat and Mass Transfer*, John Wiley & Sons, New York etc., 2002